ELSEVIER

NeuroImage

www.elsevier.com/locate/ynimg
NeuroImage 37 (2007) S89–S99

Surface rendering-based virtual intraventricular endoscopy: Retrospective feasibility study and comparison to volume rendering-based approach

Nobuyuki Nakajima,[a,b,*] Jun Wada,[b] Tamotsu Miki,[b] Jo Haraoka,[b] and Nobuhiko Hata[a]

[a]*Department of Radiology, Brigham and Women's Hospital, Boston, MA, USA*
[b]*Department of Neurosurgery, Tokyo Medical University, Tokyo, Japan*

Received 5 February 2007; revised 6 April 2007; accepted 8 April 2007
Available online 20 April 2007

Objective: **Virtual endoscopic simulations using volume rendering (VR) have been proposed as a tool for training and understanding intraventricular anatomy. It is not known whether surface rendering (SR), an alternative to VR, can visualize intraventricular and subependymal structures better and thus making the virtual endoscope more useful for simulating the intraventricular endoscopy. We sought to develop SR-virtual endoscopy and compared the visibility of anatomical structures in SR and VR using retrospective cases.**
Materials and methods: **Fourteen patients who underwent endoscopic intraventricular surgery of third ventricle enrolled the study. SR-virtual endoscopy module was developed in open-source software 3D Slicer and virtual endoscopic scenes from the retrospective cases were created. VR virtual endoscopy of the same cases was prepared in commercial software. Three neurosurgeons scored the visibility of substructures in lateral and third ventricle, arteries, cranial nerves, and other lesions**
Results**: We found that VR and SR-virtual endoscopy performed similarly in visualization of substructures in lateral and third ventricle (not significant statistically). However, the SR was statistically significantly better in visualizing subependymal arteries, cranial nerves, and other lesions ($p<0.05$, respectively).**
Conclusions: **We concluded that SR-virtual endoscopy is a promising tool to visualize critical anatomical structures in simulated endoscopic intraventricular surgery. The results lead us to propose a hybrid technique of volume and surface rendering to balance the strength of surface rendering alone in visualizing arteries, nerves and lesions, with fast volume rendering of third and lateral ventricles.**

Keywords: Virtual endoscopy; Neuroendoscopy; Third ventricle; Surface rendering; Volume rendering; Three-dimensional true fast imaging with steady-state precession

Introduction

Technological advances have allowed the introduction of intraventricular endoscopy to neurosurgery. Endoscopic intraventricular surgery has become significant choice of surgery in third ventriculostomy for non-communicating hydrocephalus (Hopf et al., 1999; Kamikawa et al., 2001; Oka et al., 1993), biopsy of intraventricular lesions (Macarthur et al., 2002; Oi et al., 2000; Souweidane et al., 2000), and fenestration of cyst (Charalampaki et al., 2005; Miki et al., 2005; Miyajima et al., 2000; Powers, 1986). However, most neurosurgeons are trained to comprehend the three-dimensional view provided by an operating microscope and are less familiar with an endoscopic view (Riegel et al., 1994). Thus, for safe application of the endoscopic technique, further experience and training are crucial (Schroeder et al., 1999, 2002; Wolfsberger et al., 2004). Otherwise, any limitation in three-dimensional anatomical comprehension might then cause abandonment of the procedure, vascular injury, oculomotor palsy, intraventricular hemorrhage, or intraparenchymal hemorrhage (Luther et al., 2005; Peretta et al., 2006; Schroeder et al., 1999).

Virtual endoscopic simulations (Robb, 2000) have been proposed as a useful tool for training and understanding intraventricular anatomy (Auer and Auer, 1998; Riegel et al., 2000; Rohde et al., 2001). Inspired by pioneering work of Auer et al., others follow with reports of virtual endoscopy for cystic lesions and fenestration of pathological membranes (Auer and Auer, 1998; Burtscher et al., 2002; Tirakotai et al., 2004) and concluded that virtual endoscopy is especially useful in identifying the lateral ventricle and surrounding critical structures. Other groups further investigated the usefulness of virtual third ventriculostomy (Burtscher et al., 2000; Freudenstein et al., 2001; Krombach et al., 2002; Riegel et al., 2000; Rohde et al., 2001) and concluded that virtual endoscopy is further appreciated in visualizing the substructure of third ventricle.

In these studies on virtual endoscopy, the computer graphics methods used were mostly volume rendering. Volume rendering is relatively simple to reconstructing endoscopic view from cranial

* Corresponding author. Department of Radiology and Surgical Planning Laboratory, Brigham and Women's Hospital, 75 Francis Street, Boston, MA 02115, USA. Fax: +1 617 582 6033.
E-mail addresses: nnakajima@bwh.harvard.edu, nakajiny@tokyo-med.ac.jp (N. Nakajima).
Available online on ScienceDirect (www.sciencedirect.com).

1053-8119/$ - see front matter © 2007 Elsevier Inc. All rights reserved.
doi:10.1016/j.neuroimage.2007.04.023

Table 1
Patient characteristics[a]

No	Sex/age (years)	Etiology	Tumor	Procedure type
1	M/29	Germinoma	Cyst and solid	Biopsy, ETV, fenestration
2	M/32	Germinoma	Solid	Biopsy, ETV
3	M/14	PPT of intermediate differentiation	Solid	Biopsy, ETV
4	M/60	Epidermoid cyst	Solid	Biopsy, ETV
5	F/29	Pineal cyst	Cyst	Fenestration, ETV
6	M/84	Unknown	Cyst and solid	Fenestration, ETV
7	F/38	Craniopharyngioma	Cyst	Fenestration, biopsy
8	M/63	Craniopharyngioma	Cyst and solid	Fenestration, biopsy
9	F/56	Craniopharyngioma	Cyst and solid	Fenestration, biopsy
10	M/49	Craniopharyngioma	Cyst and solid	Fenestration, biopsy
11	F/50	Craniopharyngioma	Cyst and solid	Fenestration, biopsy
12	F/0	Arachnoid cyst	Cyst	Fenestration
13	F/73	Metastasis	Solid	Biopsy, ETV
14	M/27	Unknown	Solid	ETV

[a] M, male; F, female; ETV, endoscopic third ventriculostomy; PPT, pineal parenchymal tumor.

magnetic resonance imaging (MRI); however, it is known to be weak in depicting subependymal structures as the related article all address (Auer and Auer, 1998; Wada et al., 2000; Wolfsberger et al., 2006). In response to similar arguments in domains other than intraventricular endoscopy, researchers have proposed surface rendering (Hayashi et al., 2003; Socha et al., 2004; Takabatake et al., 2001) and visualize hidden critical structures. However, to the best of our knowledge, a paucity of material is available on virtual intraventricular endoscopy using surface rendering, which presumably is superior in generating structures underneath the ventricle wall and is more flexible in rendering the anatomical structures.

The objective of this study, therefore, is to develop a virtual endoscopy using the surface rendering and assess its feasibility in retrospective clinical cases. We compared the surface rendering on the newly developed software, with volume rendering in terms of visualization capability.

Materials and methods

Patients

Fourteen patients who underwent endoscopic intraventricular surgery for lesions located in the third ventricle between February 2004 and February 2006 were selected. There were eight male and six female patients, aged between 0 and 84 years old (median 43.5 years). We diagnosed pineal lesions in six cases (cases 1–6), suprasellar lesions in six cases (cases 7–12), and tectal lesions in two (cases 13 and 14).

The patient's demographic characteristics are summarized in Table 1.

MR examination

All of the patients underwent MR examination in a 1.5-T MR scanner (Magnetom Symphony or Avanto; Siemens AG, Erlangen, Germany) with a head coil. We generated the virtual endoscopy from three-dimensional true fast imaging with steady-state precession (3D True FISP) after administration of contrast agent with the following parameters: repetition time 4.62 to 8.24 ms; echo time 2.31 to 4.12 ms; flip angle 60° or 70°; and slice thickness 0.8 to 1.0 mm; median scan time 4 min 27 seconds. The image contrast with True FISP is determined by T2*/T1 properties. By providing T1 contrast, True FISP can provide the enhancement effects of contrast agents in spite of the category of heavily T2-weighted imaging (Hata, 2002; Shigematsu et al., 1999). This character was useful for the anatomical delineation of tumors and normal structures.

Virtual endoscopy

Volume rendering-based virtual endoscopy

3D True FISP MR imaging data sets were transferred to a personal computer in order to construct virtual endoscopic views. Volume rendering-based virtual endoscopy (VR-virtual endoscopy) was reconstructed using image analysis software based on volume rendering techniques via ray casting (Real INTAGE, KGT Inc., Tokyo, Japan) extended to simulate virtual endoscopy

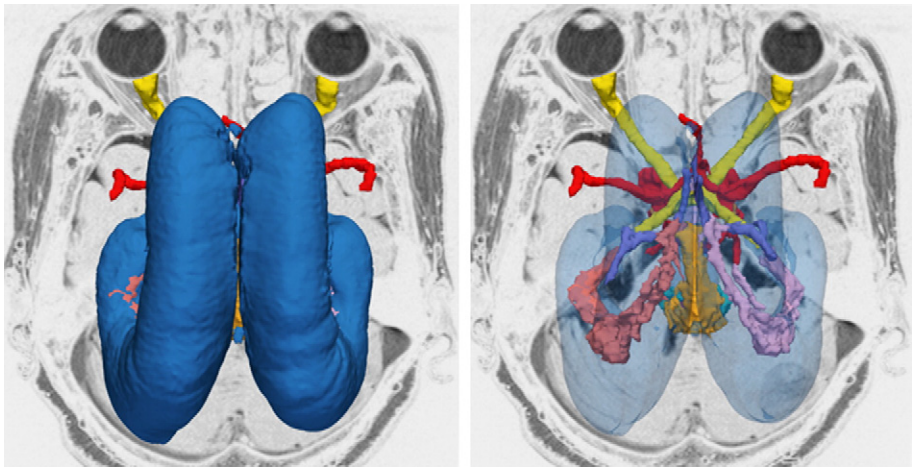

Fig. 1. Three-dimensional models of the segmented structures generated from the surface rendering-based software. Transparent view through the ventricular system allows one to observe surrounding structures which otherwise is not possible in volume-rendering-based virtual endoscopy (case 13).

(Mori et al., 2002). The operator (NN) controlled the threshold level, opacity curve, and color map to obtain optimal virtual endoscopic views.

Surface rendering-based virtual endoscopy

We modified the usage of the 3D Slicer, an image analysis and interactive visualization software, and generated surface rendering-based virtual endoscopy (SR-virtual endoscopy) (Nain et al., 2001). 3D Slicer is a software package developed and maintained by the Surgical Planning Laboratory at Brigham and Women's Hospital (Gering et al., 2001). This application package is a freely available, open-sourced tool for clinicians and scientists (www.slicer.org; see Acknowledgment for more detail). 3D True FISP MR imaging data sets were loaded into the 3D Slicer version 2.6 on a workstation (Dell Precision 470, Dell Inc., Round Rock, TX).

For all patients we created three-dimensional models of the ventricular system, including choroid plexus of lateral ventricle (uni- or bilateral), choroid plexus of the third ventricle, thalamostriate vein, septal vein, and lesion. When a tumor included both a cystic and a solid component, we distinguished cyst from solid for segmentation. Additional segmentation of the following structures was performed for the suprasellar lesion and the endoscopic third ventriculostomy: arteries, optic nerve, oculomotor nerve, abducens nerve, and pituitary (Fig. 1). Segmentation of interest was taken place by using the program's suit of editing tools, including thresholding, change island, and free-hand drawing. We obtained

Table 2
Visibility grading

Structure	n [a]	Visibility (%)								Individual comparison		Group comparison
		Volume rendering				Surface rendering						
		0	1	2	3	0	1	2	3	p value	F	m.c.
Lateral ventricle												
Foramen of Monro	42	0	0	12	88	2	2	7	88	0.6569		
Choroid plexus	42	0	2	41	57	0	0	7	93	0.0001	**	
Thalamostriate vein	42	7	17	45	31	10	21	29	40	1.0000		n.s.
Septal vein	42	17	26	36	21	48	31	12	9	0.0005	*	
Septum pellucidum	42	0	0	10	90	0	0	10	90	0.7821		
Third ventricle												
Lamina terminalis	27	0	0	22	78	0	0	30	70	0.5435		
Optic recess	24	0	4	17	79	0	4	25	71	0.6011		
Infundibular recess	24	0	4	33	63	0	13	50	37	0.0740		
Tuber cinereum	27	0	0	26	74	0	0	33	67	0.5601		n.s.
Mamillary bodies	27	0	4	33	63	0	26	37	37	0.0144	*	
Aqueduct	18	0	0	6	94	0	0	11	89	0.5601		
Posterior commissure	24	0	0	4	96	4	4	21	71	0.0303		
Habenular commissure	24	4	0	21	75	4	13	46	37	0.0277	*	
Choroid plexus	42	7	38	45	10	0	2	19	79	<0.0001	**	
Massa intermedia	39	0	0	18	82	0	5	18	77	0.3505		
Artery												
Basilar artery	42	0	0	0	100	0	0	2	98	0.3232		
P1	84	5	21	19	55	0	0	13	87	0.0002	**	
SCA	84	10	20	33	37	7	11	13	69	0.0304	*	
PcomA	84	58	14	17	11	32	6	10	52	<0.0001	**	
AcomA	42	50	21	26	3	7	5	29	59	<0.0001	**	$p<0.05$
A1	84	44	23	19	14	0	7	10	83	<0.0001	**	
A2	84	68	19	5	8	7	2	10	81	<0.0001	**	
M1	84	100	0	0	0	0	0	5	95	<0.0001	**	
ICA	84	93	0	2	5	0	0	2	98	<0.0001	**	
Cranial nerve												
Optic nerve	42	55	26	12	7	0	0	12	88	<0.0001	**	
Oculomotor nerve	84	22	13	45	20	0	0	17	83	<0.0001	**	$p<0.05$
Abducens nerve	54	70	9	15	6	34	9	22	35	0.0004	**	
Other changes												
Cyst	27	0	19	37	44	0	0	4	96	<0.0001	**	
Solid	33	33	15	24	28	9	0	3	88	<0.0001	**	
Cyst and solid	18	67	28	5	0	17	0	0	83	<0.0001	**	$p<0.05$
Catheter	6	0	0	17	83	0	0	0	100	0.3632		

[a] n, numbers of assessment by three observers; P1, first segment of posterior cerebral artery; SCA, superior cerebellar artery; PcomA, posterior communicating artery; AcomA, anterior communicating artery; A1, A1 segment of anterior cerebral artery; A2, A2 segment of anterior cerebral artery; M1, M1 segment of middle cerebral artery; ICA, internal carotid artery; F, Fisher's exact significant *p value in (0.001–0.05), **p value <0.001; m.c., Tukey multiple comparisons; n.s., not significant.

the virtual endoscopic views by changing camera position, camera orientation, visibility of each model, and opacity of each model (Jolesz et al., 1997).

Visibility grading

Three neurosurgeons from among the authors (NN, JW, and TM) evaluated the visibility of these structures using a subjective four-point grading originally proposed for virtual CT cholangiopancreatoscopy by Prassopoulos et al. (1998). In our study, we scored the visibility of cerebral structures by classifying them as follows: 0—not seen; 1—barely or not more than half of the structure seen, but the examiner considered the structures insufficient for the simulation; 2—more than half of the structure seen and the examiner considered the structures sufficient for the simulation; 3—entire structure seen. Number of score incidents for each structure in VR-based virtual endoscopy and SR-based virtual endoscopy were summed from the three neurosurgeons' score sheets, and the ratio of incidents in each score was tabulated.

We classified the anatomical structures into five major groups (lateral ventricle, third ventricle, arteries, cranial nerves, and other lesions) and argued the visibility of substructures separately.

Lateral ventricle included the foramen of Monro, choroid plexus in the lateral ventricle, thalamostriate vein, septal vein, and septum pellucidum. All 14 cases were included in the assessment of lateral ventricle. Scored substructures of the third ventricle were lamina terminalis, optic recess, infundibular recess, tuber cinereum, mamillary bodies, cerebral aqueduct, posterior commissure, habenular commissure, choroid plexus in the third ventricle, and massa intermedia. Selected substructures were assessed according to the nature of the surgery performed. Specifically, lamina terminalis, tuber cinereum, and mamillary bodies were included in the cases of pineal lesions ($n=6$, cases 1–6), tectal lesions ($n=2$, cases 13 and 14), and one suprasellar lesion ($n=1$, case 7). Optic recess, infundibular recess, and both posterior and habenular commissures were assessed in pineal ($n=6$) and tectal cases ($n=2$). The cerebral aqueduct was scored in pineal cases ($n=6$). Case 8 was excluded from scoring of massa intermedia, since we had concluded from MR images that the patient did not have the structure congenitally.

Arteries included basilar artery (BA); P1 segment of posterior cerebral artery (P1); superior cerebellar artery (SCA); posterior communicating artery (PcomA); anterior communicating artery (AcomA); A1 segment of anterior cerebral artery (A1); A2 segment of anterior cerebral artery (A2); M1 segment of middle cerebral artery (M1); and internal carotid artery (ICA). Cranial nerves included optic nerve, oculomotor nerve, and abducens nerve. All 14 cases included the scoring of these substructures except that the abducens nerve was not scored in five of the suprasellar cases (cases 7–11). Other lesions were either cystic or solid tissue, and catheter left from the previous cases. Cyst and solid means the distinction between the cystic and solid component. We selected the structures for scoring based on MR image findings.

We performed two sets of statistical analysis to compare the visibility of thirty-one individual structures and five group sets with these structures. The five groups were lateral ventricle, third ventricle, arteries, cranial nerves, and other lesions all described with their substructures above. The visibilities of individual structures were compared using Fisher's exact test, and the groups were compared by Tukey multiple comparisons test. In both analyses, the confidence interval was set to 95% or $p<0.05$. We used the statistical software: SAS 9.1 (SAS Institute, Cary, NC).

Results

Virtual endoscopy was feasible in all 14 patients using both VR-virtual endoscopy and SR-virtual endoscopy. VR-virtual endoscopy was generated within 15 min after loading an image data set. On the other hand, segmentation of interest structures for the SR-virtual endoscopy required 170–370 min (median 234 min) excluding the first four cases (cases 1, 8, 12, and 13).

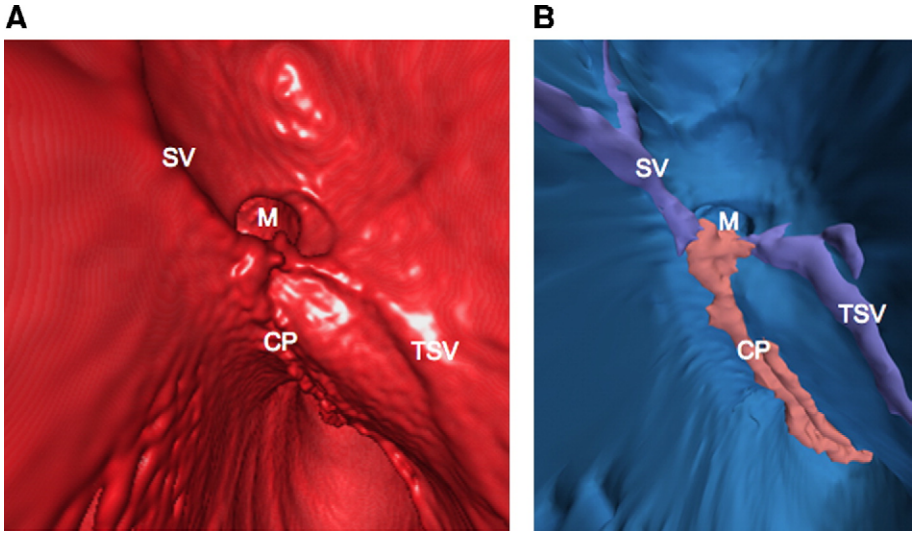

Fig. 2. Comparison of volume rendering-based virtual endoscopy (A) and surface rendering-based virtual endoscopy (B) near right lateral ventricle (case 13). Both virtual endoscopic images observe the right lateral ventricle via anterior horn. Virtual endoscopy shows the foramen of Monro, choroid plexus, thalamostriate vein, and septal vein marked as M, CP, TSV, and SV respectively. Observers scored highest visibility in both view assessing the visibility of the substructures.

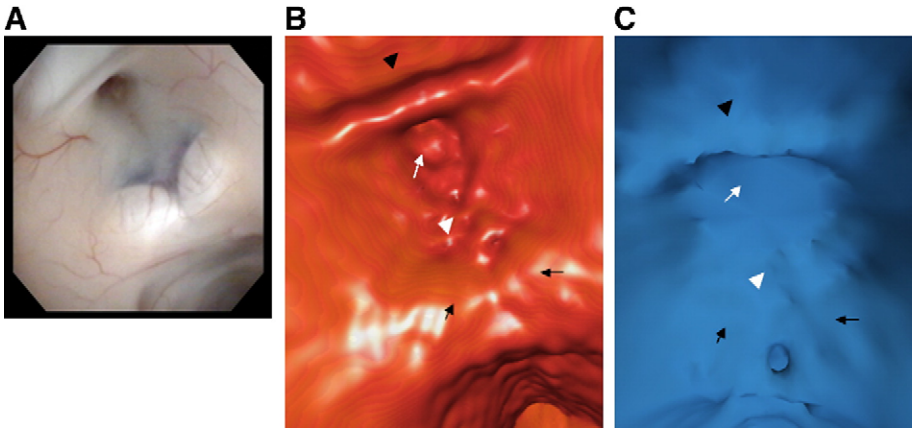

Fig. 3. Comparison of volume rendering-based virtual endoscopy and surface rendering-based virtual endoscopy near the anterior part of the third ventricle (case 13). (A) Intraoperative endoscopic image by flexible videoscope. (B) Volume rendering-based virtual endoscopy. (C) Surface rendering-based virtual endoscopy. The mamillary bodies had a higher visibility grade in the volume rendering-based virtual endoscopy than in the surface rendering-based virtual endoscopy. Mamillary bodies, black arrow; tuber cinereum, white arrowhead; infundibular recess, white arrow; optic recess, black arrowhead.

Visibility grading

The results of the visibility grading and statistical analysis are summarized in Table 2.

Lateral ventricle

Representative virtual endoscopic views from VR-virtual endoscopy and SR-virtual endoscopy are shown in Fig. 2. Foramen of Monro, choroid plexus, and septum pellucidum were rated highest among the substructures of lateral ventricle in both VR- and SR-virtual endoscopy (grade 2 and above, 95–100%), but ependymal veins are rated lower than the other three (grade 2 and above, 21–76%). In Fisher's exact test (Table 2), the choroids plexus was more visible in SR-virtual endoscopies than in VR-virtual endoscopies and the septal vein was more visible in VR-virtual endoscopies than in SR-virtual endoscopies.

However, VR-virtual endoscopy and SR-virtual endoscopy are similar in the ability to visualize the substructures in the group comparison. There is room for improvement in ependymal vein visualization in both types of virtual endoscopy.

Third ventricle

In the floor of the third ventricle (Fig. 3), VR-virtual endoscopy and SR-virtual endoscopy had similar grades and scored relatively

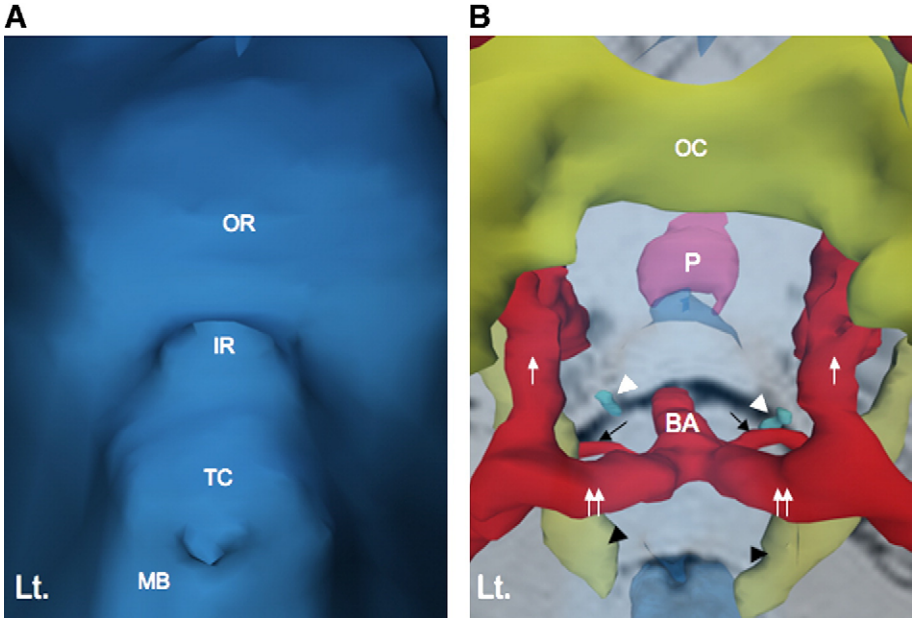

Fig. 4. The floor of the third ventricle and prepontine critical structures in surface rendering-based virtual endoscopy (case 5). (A) The floor of the third ventricle. (B) The transparent image with the same virtual endoscopic field of the left image reveals the relationships between the floor of the third ventricle and the prepontine structures. Lt, left; MB, mamillary bodies; TC, tuber cinereum; IR, infundibular recess; OR, optic recess; OC, optic chiasm; P, pituitary; BA, basilar artery; posterior communicating artery, white arrow; superior cerebellar artery, black arrow; P1 segment of the posterior cerebral artery, white double arrows; oculomotor nerve, black arrowhead; abducens nerve, white arrowhead.

well (grade 2 and above, 74–100%). The mamillary bodies had a higher visibility grade in the VR-virtual endoscopy than in the SR-virtual endoscopy with the Fisher's exact significant. VR-virtual endoscopy and SR-virtual endoscopy also had similar grades in the visibility of the posterior part of the third ventricle except for the habenular commissure. One can notice that the visibility of the choroid plexus in the third ventricle was poorer in VR-virtual endoscopy than in SR-virtual endoscopy with the Fisher's exact significant.

In multiple comparisons analysis (Table 2) to compare the visibility by the group, VR-virtual endoscopy and SR-virtual endoscopy are similar in the ability to visualize the substructures of third ventricle group.

Arteries

In all cases, the basilar arteries were well visible by VR-virtual endoscopy and SR-virtual endoscopy and all three observers gave score 2 and higher in 100% of the cases. However, other arteries (P1, SCA, PcomA, AcomA, A1, A2, M1, and ICA) were statistically significantly well visualized in SR-virtual endoscopy. The strength of SR-virtual endoscopy was its ability to reveal the artery by rendering the ventricle wall transparent, as is shown in Fig. 4. We could visualize other arteries in VR-virtual endoscopy; however, this was possible only by removing the ventricle floor and moving the camera closer to the artery, as is shown in Fig. 5. AcomA, A1 and A2 were hardly visible in VR-virtual endoscopy but slightly visible if the lamina terminalis were removed from view (grade 2 and above, 13–33%). On the other hand, in SR-virtual endoscopy, AcomA, A1, and A2 were visualized through the lamina terminalis (grade 2 and above, 88–93%). In three cases (2, 4, and 14), the thin cistern made segmentation of SCA, PcomA, AcomA, A1, and A2 difficult and visualization of these substructures were poor also in SR-virtual endoscopy.

In the group comparison of visualizing arteries (Table 2), the SR-virtual endoscopy is statistically significantly better than the VR-virtual endoscopy.

Cranial nerves

The optic nerves were visualized poor in VR-virtual endoscopy views; however, SR-virtual endoscopy had excellent delineation of the optic nerve with the Fisher's exact significant, except for two cases. Those cases were case 10, where the patient had a mixed complicated suprasellar lesion, and case 14, where the patient had a tight cistern due to ventriculomegaly. VR-virtual endoscopy revealed the oculomotor nerves less than visualized SR-virtual endoscopy with which the observers scored 2 and more in all the

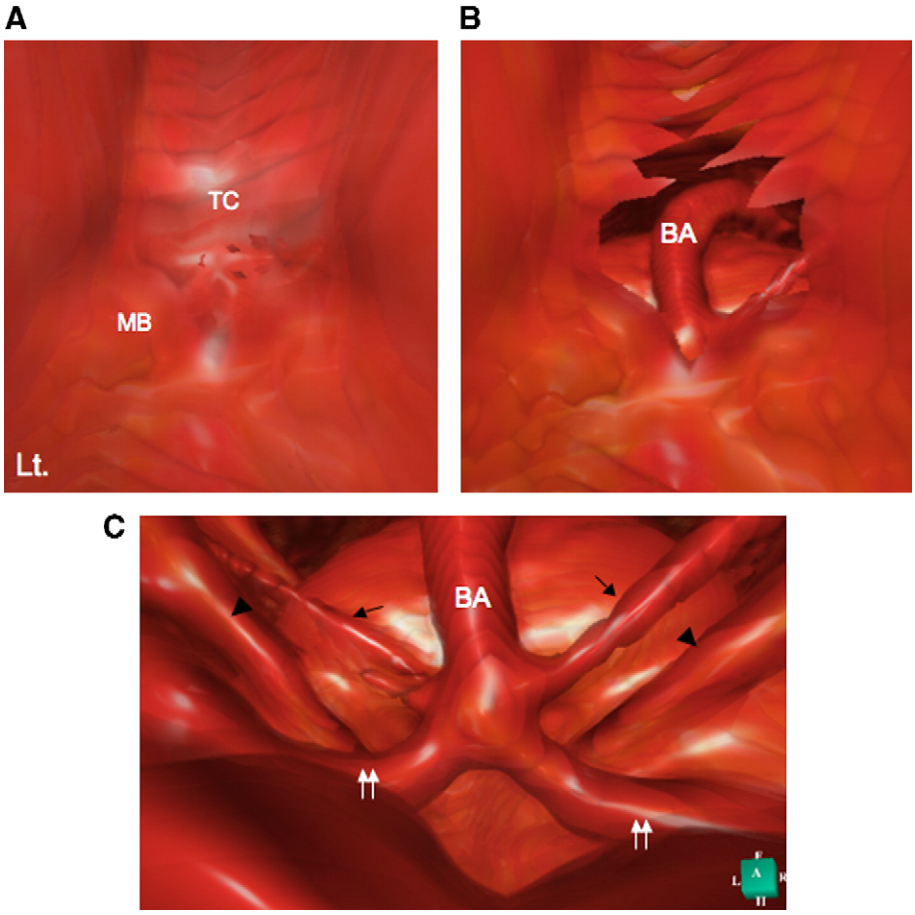

Fig. 5. The floor of the third ventricle and prepontine critical structures in volume rendering-based virtual endoscopy (case 6). (A) The floor of the third ventricle. (B) The floor was removed by changing the threshold curve, but the view of the prepontine space is limited. (C) We need to move the camera closer to visualize the prepontine structures. Lt, left; MB, mamillary bodies; TC, tuber cinereum; BA, basilar artery; superior cerebellar artery, black arrow; P1 segment of the posterior cerebral artery, white double arrows; oculomotor nerve, black arrowhead.

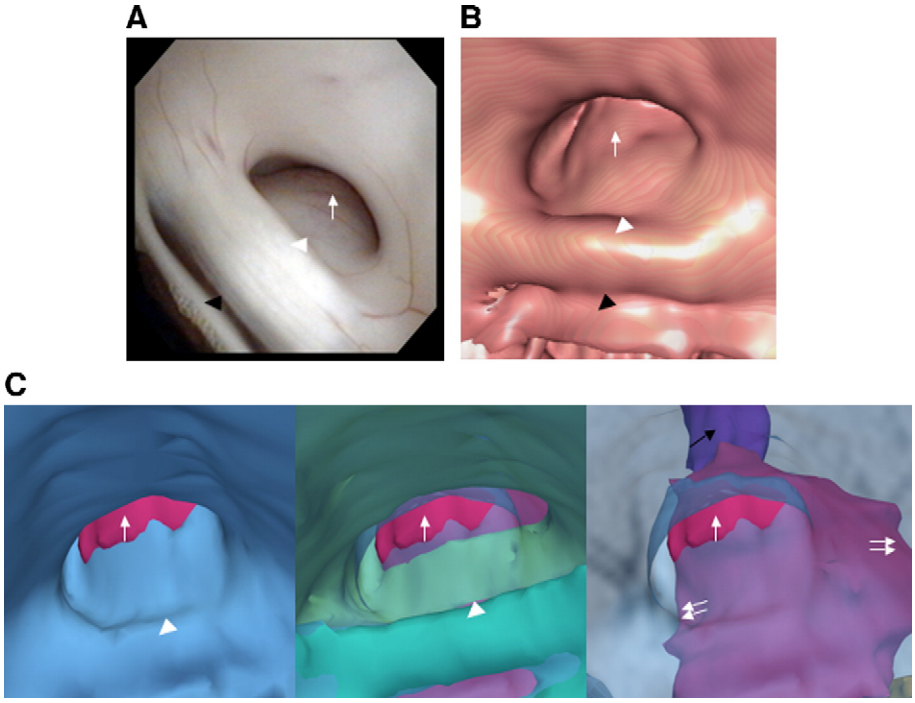

Fig. 6. Visualization of the subependymal extension of the tumor (case 13). (A) The real intraoperative image (flexible videoscope) presents the cerebral aqueduct obstructed by the tectal tumor. (B) Volume rendering-based virtual endoscopy provides the similar image to the real intraoperative image. (C) Surface rendering-based virtual endoscopy reveals the subependymal extension of the tumor by changing the opacity and visibility of the other structures. Tumor (white arrow); posterior commissure (white arrowhead); habenular commissure (black arrowhead); cerebral aqueduct behind the tumor (black arrow).

cases. It should be noted the spatial relationship between the floor and oculomotor nerve was hard to comprehend with VR-virtual endoscopy, whereas SR-virtual endoscopy showed them well. Although the abducens nerves were statistically visualized in SR-virtual endoscopy, the results were not sufficient for the visibility. The abducens nerves were sufficiently visible in 21% of instances of VR-virtual endoscopy and 57% of SR-virtual endoscopy. In both techniques, the cerebralspinal fluid flow specific artifact of the original MRI obstructed the identification of the abducens nerve, especially in cases with a narrow prepontine cistern.

In the group comparison of visualizing cranial nerves (Table 2), the SR-virtual endoscopy is statistically significantly better than the VR-virtual endoscopy.

Other lesions

Lesions (cyst, solid, and distinction between cyst and solid) were significantly visualized well in SR-virtual endoscopy. Nine cases had a cyst, and VR-virtual endoscopy scored relatively well: in one case with a suprasellar arachnoid cyst (case 12) whose tissue content had the same image intensity as cerebral spinal fluid, the cyst was assigned score 1. VR-virtual endoscopy performed also well in cases with simple solid lesion (cases 2–4, 13, and 14). However, VR-virtual endoscopy could not depict anatomy of the lesions composed of both solid and cystic components ($n=6$) scored 1 and less in all of these cases. SR-virtual endoscopy performed well in solid and cystic lesion cases except for one case with craniopharyngioma (case 9), where the solid component could not be identified in the original MRI. In eight cases (cases 1–4, 6, 7, 13, and 14), tumor lesion partially extended to the extra-third ventricle. Although VR-virtual endoscopy could not reveal the extension in all eight cases, SR-virtual endoscopy showed its strength in visualizing the subependymal extension of the tumor using a transparent view in all eight cases (Fig. 6).

In the group comparison of the other lesions (Table 2), the SR-virtual endoscopy is statistically significantly better than the VR-virtual endoscopy.

Illustrative case of virtual endoscopy

Subependymal extension of tumor (case 1, male, 27 years old)

MR images of this patient had shown cystic and solid tumor extending from pineal, through the tegmentum, and then to right thalamus. In addition, the tumor invaded the massa intermedia (Fig. 7A). Endoscopic fenestration of the cyst was performed to collect solid tissue, followed by biopsy of the right thalamus lesion through the lateral wall of the third ventricle. The histological results of both two biopsies showed pure germinoma.

In comparing the video snapshots of endoscopic images (Fig. 7B), we found that VR-virtual endoscopy was helpful only in showing the swollen tegmentum (Fig. 7C), but SR-virtual endoscopy was more helpful when the tumor extended to right thalamus and massa intermedia. This finding of SR-virtual endoscopy would be of use in identifying tumors behind the third ventricle wall and in avoiding damage to critical structures (Fig. 7D).

Distinction between cyst and solid component (case 6, male, 84 years old)

MRI findings in this patient suggested a large cyst in the pineal lesion and a solid lesion in the superior vermis (Figs. 8A and B). Endoscopic fenestration of the cyst and third ventriculostomy were performed, and sampling of the tissue from the lesion was attempted.

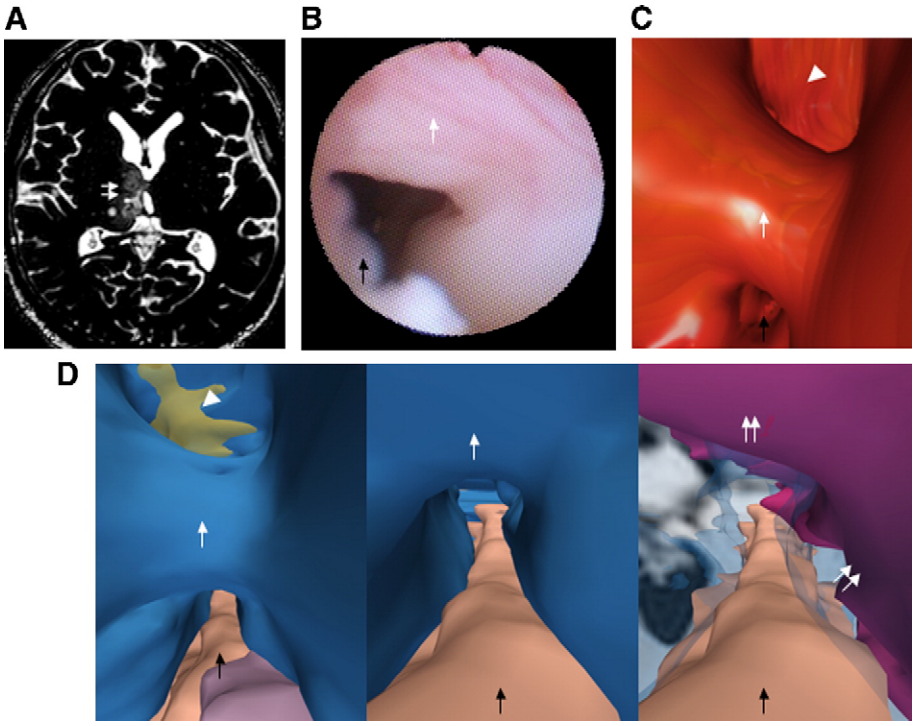

Fig. 7. A 27-year-old male with a pineal germinoma (case 1). (A) Contrast-enhanced 3D True FISP image reveals the tumor extending to the right thalamus (white double arrows). In addition, the tumor invades the massa intermedia. (B) The real intraoperative image (flexible fiberscope) shows the massa intermedia (white arrow), right lateral wall of the third ventricle and choroid plexus (black arrow). (C) This volume rendering-based virtual endoscopy only shows the swollen tegmentum (white arrowhead). We cannot confirm the subependymal tumor behind the lateral wall and massa intermedia (white arrow). (D) Left image; this surface rendering-based virtual endoscopy shows the massa intermedia (white arrow), choroid plexus in the roof of the third ventricle (black arrow), and the swollen tegmentum due to the cystic component (white arrowhead). Middle image; the camera is approaching the supra-massa intermedia space. Right image; by changing the opacity of the ventricle, we can identify the subependymal extension of the tumor (white double arrows). Middle and right images show the same virtual endoscopic field.

Due to incorrect orientation during the procedure (Fig. 8C), a limited tissue sample was collected only from the cystic wall, and no solid tissue was collected. We therefore did not have conclusive information on pathology.

Intra-cystic examination using VR-virtual endoscopy also revealed veins; however, differentiating the solid tissue from the cystic tissue was difficult (Fig. 8D). On the other hand, SR-virtual endoscopy provided helpful observation of solid tissue intra-cystically (Fig. 8E).

Discussion

Results of this study indicate that SR-virtual endoscopy of endoscopic intraventricular surgery is feasible and offers promise as a method to visualize critical structures. We found that SR-virtual endoscopy is on par with VR-virtual endoscopy in visualization of substructures in the lateral and third ventricle and yet better than VR-virtual endoscopy at visualizing arteries, cranial nerves, and solid and cystic lesions.

These findings are consistent with and expand upon those in prior reports. Other groups reporting on virtual endoscopy in neurosurgery have mainly used MRI images. Those studies include visualization of normal and pathological ventricular anatomy (Auer and Auer, 1998; Burtscher et al., 1999; Freudenstein et al., 2001; Krombach et al., 2002; Riegel et al., 2000; Shigematsu et al., 1998b; Wada et al., 2000), basilar artery (Burtscher et al., 2000; Kakizawa et al., 2003; Rohde et al., 2001), intraventricular cyst (Burtscher et al., 2002), vestibular schwannoma (Kakizawa et al., 2003; Shigematsu et al., 1998a), trigeminal neuralgia (Akimoto et al., 2002), facial spasm (Kakizawa et al., 2003; Shigematsu et al., 1998a), and tinnitus (Nowe et al., 2004).

Our approach is unique in its capacity to visualize anatomy and its subsurface structure. Auer and Auer (1998) reported that their difficulty in visualizing the components of brain vascular simultaneously harms the usefulness of volume rendering. They also concluded that the lack of major vascular landmarks, such as the thalamostriate vein and the septal vein "limits the applicability as a teaching and training tool." Our approach using surface rendering addresses this issue by making the anatomy transparent. The merit of this approach has been proven in our visibility study.

This study implies SR-virtual endoscopy of intraventricular surgery is useful in three ways.

First, it is useful in understanding the spatial relationships between the floor of the third ventricle and the prepontine structures. In this series, endoscopic third ventriculostomy was performed in eight cases. SR-virtual endoscopy revealed the relationships between the floor of the third ventricle and the prepontine structures in all eight cases without moving the position of camera into the prepontine cistern, as has to happen with VR-virtual endoscopy. Understanding critical structures such as the basilar artery, posterior cerebral artery, and the oculomotor nerve in the prepontine cistern is essential in endoscopic third ventriculostomy. However, it is often difficult to visualize these anatomical structures from the endoscopic view due in large part to the variability of anatomy. Virtual endo-

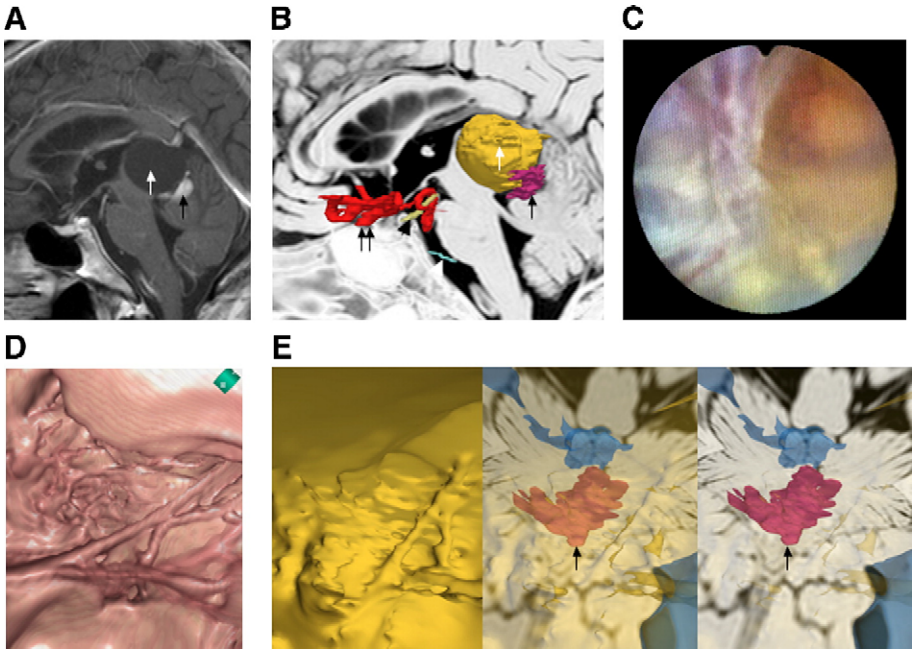

Fig. 8. An 84-year-old male with a pineal lesion (case 6). (A) Contrast-enhanced T1-weighted sagittal image reveals the large cyst (white arrow) in the pineal lesion and a solid component (black arrow) in the superior vermis. (B) Three-dimensional models of cyst (white arrow), solid component (black arrow), arteries (black double arrows), left oculomotor nerve (black arrowhead), and left abducens nerve (white arrowhead) are registered with the original 3D True FISP sagittal image. (C) The real intraoperative image (flexible fiberscope) shows the view of the intra-cyst. (D) The view of the intra-cyst using volume rendering-based virtual endoscopy reveals the veins; however, differentiating the location of the solid tissue is difficult. (E) The intra-cystic view is shown using surface rendering-based virtual endoscopy. By changing the opacity of the cyst, we can identify the location of the solid tissue from the intra-cyst (black arrow). Left, middle, and right images show the same virtual endoscopic field.

scopy may enable us to simulate the realistic endoscopic view before or even during the surgery and also provides us a see-through image of the third ventricle floor including the prepontine cistern. This advantage was confirmed when we compared SR-virtual endoscopy and VR-virtual endoscopy.

Second, SR-virtual endoscopy may be useful to visualize a subependymal extension of a tumor that in standard current practice can only be speculated upon from the swelling of the ventricle wall. The ability to alter the opacity of anatomical structures and differentiate them by color in SR-virtual endoscopy is especially useful in assessing the extension of a tumor.

Third, SR-virtual endoscopy may be useful to distinguish solid tissue from cystic tissue when taking biopsy samples. The endoscopic view from inside the cystic component often lacks landmarks for orientation, a common cause of mis-sampling or incompletion. In SR-virtual endoscopy, we can also identify the basilar artery, the oculomotor nerve, and the optic nerve behind the solid and cystic tissue.

Additional advantages of the information gathered through our method are reduced surgical times and increased accuracy, which eventually may lead to fewer complications (Schroeder et al., 2002). With the assistance of virtual endoscopy, more procedures may be completed without stopping because of an adverse event during surgery (Peretta et al., 2006).

Some limitations of SR-virtual endoscopy presented in this paper are that it requires relatively high operator participation and a relatively long amount of time for constructing three-dimensional graphics models (median 234 min per case). VR-virtual endoscopy may be a suitable choice for a surgical scenario where the lateral and third ventricle are the only substructures that need to be identified since the time required for generating VR-virtual endoscopy is relatively short and operator intervention is minimal. However, most intraventricular endoscopy requires identification of arteries and cranial nerves, which were found to be more visible through SR-virtual endoscopy than VR-virtual endoscopy. The challenge therefore is to shorten the time required for preparing the virtual endoscopy using advanced graphics techniques.

Although we did not evaluate the realness of the virtual endoscopy, we were impressed that VR-virtual endoscopy might be more realistic than SR-virtual endoscopy. Objects of similar image intensities will appear similar to each other on VR-virtual endoscopy. SR-virtual endoscopy does have the advantage of color-coding individual anatomical structures to enable clinicians to understand the three-dimensional anatomy even when it is away from the actual endoscopic view.

In this study we focused on assuming virtual endoscopy as a planning and simulation tool for a particular case. However, one of the greatest uses of this proposed technique could be as a training tool. In addition to providing brightly colored segmentations of areas, it would be important that SR-virtual endoscopy is capable of providing realistic visualizations, as has to happen with VR-virtual endoscopy. Its capabilities as a training tool more than offset any time required to process images.

In SR-virtual endoscopy, segmentation is an important process. Although we did not evaluate the accuracy of segmentation in this study, in three cases the thin cistern made segmentations of the arteries difficult. Visualization of these structures was also poor in SR-virtual endoscopy. SR-virtual endoscopy would also be biased by the experience of image processing staff. Warfield et al. (2004) claimed that the performance of raters (human or algorithmic),

who generate segmentations of medical images, has been difficult to quantify because of the difficulty of obtaining a known true segmentation for clinical data. In our next phase of study, we will conduct a separate set of studies to assess inter-rater variability of segmentation in neuroendoscopic simulation and training. Additionally, we will predict its impact on accuracy in surgical guidance.

A possible solution to overcome these issues, i.e. processing time, realistic images on SR-virtual endoscopy, and segmentation errors, is hybrid rendering using both VR- and SR-virtual endoscopy. By merging the volume and surface rendering approaches, we could compensate for each of their strengths and weaknesses. Wolfsberger et al. proposed CT-based virtual endoscopy blended with data extracted from MRIs on tumor, internal carotid artery, pituitary grand, and cerebral cistern (Neubauer et al., 2005; Wolfsberger et al., 2004; Wolfsberger et al., 2006). This approach generates a model more quickly by focusing on the relatively easy segmentation of anatomy from CT images, combined with artery and soft tissue structures visible only from MRI. Inclusion of MR angiography to source images may impact the visualization quality of both VR- and SR-virtual endoscopy by further enhancing the arteries that is critical in intraventricular endoscopic simulation. Additionally, the technique of texture-mapping might be useful instead of color-coding to emphasize the reality of SR-virtual endoscopy (Jin et al., 2006). Overall, we believe that combining these rendering approaches will be the most useful to clinical practice.

Conclusion

We found that surface rendering-based virtual endoscopy is a promising tool to visualize critical anatomical structures in simulated endoscopic intraventricular surgery. The results lead us to propose a hybrid technique of volume and surface rendering to balance the strength of surface rendering alone in visualizing arteries, nerves and lesions, with fast volume rendering of third and lateral ventricles. However, this proposition warrants further examination.

Acknowledgments

This publication was made possible by Grant Number 5P01CA067165 and 5U41RR019703 from NIH. Its contents are solely the responsibility of the authors and do not necessarily represent the official views of the NIH.

The virtual endoscope software, 3D Slicer, developed and applied in this study is freely available to public with source codes. Please visit www.slicer.org for more information about the 3D Slicer.

References

Akimoto, H., Nagaoka, T., Nariai, T., Takada, Y., Ohno, K., Yoshino, N., 2002. Preoperative evaluation of neurovascular compression in patients with trigeminal neuralgia by use of three-dimensional reconstruction from two types of high-resolution magnetic resonance imaging. Neurosurgery 51, 956–961 (discussion 961-952).

Auer, L.M., Auer, D.P., 1998. Virtual endoscopy for planning and simulation of minimally invasive neurosurgery. Neurosurgery 43, 529–537 (discussion 537-548).

Burtscher, J., Dessl, A., Maurer, H., Seiwald, M., Felber, S., 1999. Virtual neuroendoscopy, a comparative magnetic resonance and anatomical study. Minim. Invasive Neurosurg. 42, 113–117.

Burtscher, J., Dessl, A., Bale, R., Eisner, W., Auer, A., Twerdy, K., Felber, S., 2000. Virtual endoscopy for planning endoscopic third ventriculostomy procedures. Pediatr. Neurosurg. 32, 77–82.

Burtscher, J., Bale, R., Dessl, A., Eisner, W., Twerdy, K., Sweeney, R.A., Felber, S., 2002. Virtual endoscopy for planning neuro-endoscopic intraventricular surgery. Minim. Invasive Neurosurg. 45, 24–31.

Charalampaki, P., Filippi, R., Welschehold, S., Conrad, J., 2005. Endoscopic and endoscope-assisted neurosurgical treatment of suprasellar arachnoidal cysts (Mickey Mouse cysts). Minim. Invasive Neurosurg. 48, 283–288.

Freudenstein, D., Bartz, D., Skalej, M., Duffner, F., 2001. New virtual system for planning of neuroendoscopic interventions. Comput. Aided Surg. 6, 77–84.

Gering, D.T., Nabavi, A., Kikinis, R., Hata, N., O'Donnell, L.J., Grimson, W.E., Jolesz, F.A., Black, P.M., Wells III, W.M., 2001. An integrated visualization system for surgical planning and guidance using image fusion and an open MR. J. Magn. Reson. Imaging 13, 967–975.

Hata, Y., 2002. Clinical application of True FISP to contrast-enhanced MR imaging. Japanese J. Magn. Reson. Med. 22, 157–165.

Hayashi, Y., Mori, K., Hasegawa, J., Suenaga, Y., Toriwaki, J., 2003. A method for detecting undisplayed regions in virtual colonoscopy and its application to quantitative evaluation of fly-through methods. Acad. Radiol. 10, 1380–1391.

Hopf, N.J., Grunert, P., Fries, G., Resch, K.D., Perneczky, A., 1999. Endoscopic third ventriculostomy: outcome analysis of 100 consecutive procedures. Neurosurgery 44, 795–804 (discussion 804-796).

Jin, W., Lim, Y.J., Singh, T.P., De, S., 2006. Use of surgical videos for realistic simulation of surgical procedures. Stud. Health Technol. Inform. 119, 234–239.

Jolesz, F.A., Lorensen, W.E., Shinmoto, H., Atsumi, H., Nakajima, S., Kavanaugh, P., Saiviroonporn, P., Seltzer, S.E., Silverman, S.G., Phillips, M., Kikinis, R., 1997. Interactive virtual endoscopy. Am. J. Roentgenol. 169, 1229–1235.

Kakizawa, Y., Hongo, K., Takasawa, H., Miyairi, Y., Sato, A., Tanaka, Y., Kobayashi, S., 2003. "Real" three-dimensional constructive interference in steady-state imaging to discern microneurosurgical anatomy. Technical note J. Neurosurg. 98, 625–630.

Kamikawa, S., Inui, A., Kobayashi, N., Kuwamura, K., Kasuga, M., Yamadori, T., Tamaki, N., 2001. Endoscopic treatment of hydrocephalus in children: a controlled study using newly developed Yamadori-type ventriculoscopes. Minim. Invasive Neurosurg. 44, 25–30.

Krombach, A., Rohde, V., Haage, P., Struffert, T., Kilbinger, M., Thron, A., 2002. Virtual endoscopy combined with intraoperative neuronavigation for planning of endoscopic surgery in patients with occlusive hydrocephalus and intracranial cysts. Neuroradiology 44, 279–285.

Luther, N., Cohen, A., Souweidane, M.M., 2005. Hemorrhagic sequelae from intracranial neuroendoscopic procedures for intraventricular tumors. Neurosurg. Focus 19, E9.

Macarthur, D.C., Buxton, N., Punt, J., Vloeberghs, M., Robertson, I.J., 2002. The role of neuroendoscopy in the management of brain tumours. Br. J. Neurosurg. 16, 465–470.

Miki, T., Wada, J., Nakajima, N., Inaji, T., Akimoto, J., Haraoka, J., 2005. Operative indications and neuroendoscopic management of symptomatic cysts of the septum pellucidum. Childs Nerv. Syst. 21, 372–381.

Miyajima, M., Arai, H., Okuda, O., Hishii, M., Nakanishi, H., Sato, K., 2000. Possible origin of suprasellar arachnoid cysts: neuroimaging and neurosurgical observations in nine cases. J. Neurosurg. 93, 62–67.

Mori, K., Suenaga, Y., Toriwaki, J., 2002. Fast volume rendering based on software optimization using multimedia instructions PC platform. Proceedings of Computer Assisted Radiology and Surgry, 782–787.

Nain, D., Haker, S., Kikinis, R., Grimson, W.E., 2001. An Interactive Virtual Endoscopy Tool. Interactive Medical Image Visualization and Analysis. Utrecht, Netherland.

Neubauer, A., Wolfsberger, S., Forster, M.T., Mroz, L., Wegenkittl, R.,

Buhler, K., 2005. Advanced virtual endoscopic pituitary surgery. IEEE Trans. Vis. Comput. Graph. 11, 497–507.

Nowe, V., Michiels, J.L., Salgado, R., De Ridder, D., Van de Heyning, P.H., De Schepper, A.M., Parizel, P.M., 2004. High-resolution virtual MR endoscopy of the cerebellopontine angle. Am. J. Roentgenol. 182, 379–384.

Oi, S., Shibata, M., Tominaga, J., Honda, Y., Shinoda, M., Takei, F., Tsugane, R., Matsuzawa, K., Sato, O., 2000. Efficacy of neuroendoscopic procedures in minimally invasive preferential management of pineal region tumors: a prospective study. J. Neurosurg. 93, 245–253.

Oka, K., Yamamoto, M., Ikeda, K., Tomonaga, M., 1993. Flexible endoneurosurgical therapy for aqueductal stenosis. Neurosurgery 33, 236–242 (discussion 242-233).

Peretta, P., Ragazzi, P., Galarza, M., Genitori, L., Giordano, F., Mussa, F., Cinalli, G., 2006. Complications and pitfalls of neuroendoscopic surgery in children. J. Neurosurg. 105, 187–193.

Powers, S.K., 1986. Fenestration of intraventricular cysts using a flexible, steerable endoscope and the argon laser. Neurosurgery 18, 637–641.

Prassopoulos, P., Raptopoulos, V., Chuttani, R., McKee, J.D., McNicholas, M.M., Sheiman, R.G., 1998. Development of virtual CT cholangiopancreatoscopy. Radiology 209, 570–574.

Riegel, T., Hellwig, D., Bauer, B.L., Mennel, H.D., 1994. Endoscopic anatomy of the third ventricle. Acta Neurochir., Suppl. 61, 54–56.

Riegel, T., Alberti, O., Retsch, R., Shiratori, V., Hellwig, D., Bertalanffy, H., 2000. Relationships of virtual reality neuroendoscopic simulations to actual imaging. Minim Invasive Neurosurg. 43, 176–180.

Robb, R.A., 2000. Virtual endoscopy: development and evaluation using the visible human datasets. Comput. Med. Imaging Graph. 24, 133–151.

Rohde, V., Krombach, G.A., Struffert, T., Gilsbach, J.M., 2001. Virtual MRI endoscopy: detection of anomalies of the ventricular anatomy and its possible role as a presurgical planning tool for endoscopic third ventriculostomy. Acta Neurochir. (Wien.) 143, 1085–1091.

Schroeder, H.W., Warzok, R.W., Assaf, J.A., Gaab, M.R., 1999. Fatal subarachnoid hemorrhage after endoscopic third ventriculostomy Case report J. Neurosurg. 90, 153–155.

Schroeder, H.W., Niendorf, W.R., Gaab, M.R., 2002. Complications of endoscopic third ventriculostomy. J. Neurosurg. 96, 1032–1040.

Shigematsu, Y., Korogi, Y., Hirai, T., Okuda, T., Ikushima, I., Sugahara, T., Liang, L., Ge, Y., Takahashi, M., 1998a. Virtual MRI endoscopy of the intracranial cerebrospinal fluid spaces. Neuroradiology 40, 644–650.

Shigematsu, Y., Korogi, Y., Hirai, T., Okuda, T., Sugahara, T., Liang, L., Ge, Y., Takahashi III, M., 1998b. New developments: 2. Virtual MR endoscopy in the central nervous system. J. Magn. Reson. Imaging 8, 289–296.

Shigematsu, Y., Korogi, Y., Hirai, T., Okuda, T., Ikushima, I., Sugahara, T., Liang, L., Takahashi, M., 1999. Contrast-enhanced CISS MRI of vestibular schwannomas: phantom and clinical studies. J. Comput. Assist. Tomogr. 23, 224–231.

Socha, M., Duplaga, M., Turcza, P., 2004. Methods of bronchial tree reconstruction and camera distortion corrections for virtual endoscopic environments. Stud. Health Technol. Inform. 105, 285–295.

Souweidane, M.M., Sandberg, D.I., Bilsky, M.H., Gutin, P.H., 2000. Endoscopic biopsy for tumors of the third ventricle. Pediatr. Neurosurg. 33, 132–137.

Takabatake, H., Mori, M., Natori, H., Mori, K., Toriwaki, J., 2001. Virtual bronchoscope system. Rinsho Byori 49, 352–355.

Tirakotai, W., Bozinov, O., Sure, U., Riegel, T., Bertalanffy, H., Hellwig, D., 2004. The evolution of stereotactic guidance in neuroendoscopy. Child's Nerv. Syst. 20, 790–795.

Wada, J., Nakajima, N., Miki, T., Ito, H., 2000. Periventricular anatomy viewed from inside the ventricles. In Proceedings of Surgical Anatomy for Microneurosurgery 12, 44–53 [In Japanese].

Warfield, S.K., Zou, K.H., Wells, W.M., 2004. Simultaneous truth and performance level estimation (STAPLE): an algorithm for the validation of image segmentation. IEEE Trans. Med. Imaging 23, 903–921.

Wolfsberger, S., Forster, M.T., Donat, M., Neubauer, A., Buhler, K., Wegenkittl, R., Czech, T., Hainfellner, J.A., Knosp, E., 2004. Virtual endoscopy is a useful device for training and preoperative planning of transsphenoidal endoscopic pituitary surgery. Minim. Invasive Neurosurg. 47, 214–220.

Wolfsberger, S., Neubauer, A., Buhler, K., Wegenkittl, R., Czech, T., Gentzsch, S., Bocher-Schwarz, H.G., Knosp, E., 2006. Advanced virtual endoscopy for endoscopic transsphenoidal pituitary surgery. Neurosurgery 59, 1001–1009 (discussion 1009-1010).